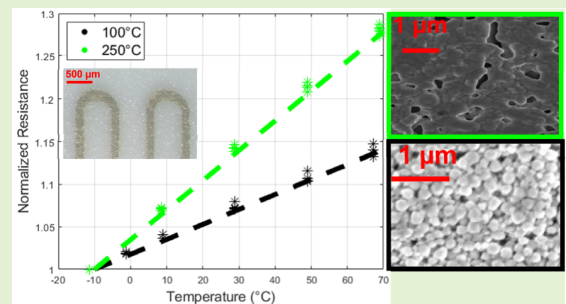


Evaluation of the Curing Process Effects on the TCR of Temperature Sensors Printed by Aerosol Jet Printing

Tiziano Fapanni¹, Hatem ElBidweihy², Dario Zappa¹, Elisabetta Comini, Emilio Sardini¹, *Member, IEEE*, and Mauro Serpelloni¹, *Senior Member, IEEE*

Abstract—Temperature sensors have been widely developed to control the course of diseases, improve haptic feelings, and in multisensing systems to compensate for the output of other temperature-sensitive sensors. The use of additive manufacturing to produce resistive temperature detectors (RTDs) with reduced dimensions and bulkiness is attracting great interest. Among the relevant process parameters and design choices, the curing process must be considered. In this work, two different commercial metallic-based materials are cured at various temperatures to evaluate the differences in their microscopic and macroscopic behavior. The sensors were designed, developed, and evaluated for their temperature coefficient of resistance (TCR) at different curing temperatures using a programmable climatic chamber. A scanning electron microscope (SEM) has been used to microscopically inspect the sensing structures with respect to the different curing temperatures. The results show insightful correlations between the macroscopic and microscopic behavior of the used inks as well as the performance of the sensors. In particular, increasing the curing temperature decreased the room temperature resistance in all the samples by up to 70% and increased the sensitivity by up to 95%. These findings will help propose better processes as well as design choices for the development of printed resistive temperature sensors.

Index Terms—Aerosol jet printing (AJP), curing process evaluation, temperature sensors.



I. INTRODUCTION

EVEN though temperature sensors are now widespread and used in a plethora of applications, they are still objects of vivid interest in the research community, presenting an exponential growth in the number of published articles from the 1980s to the present day.

Monitoring of physiological parameters in the healthcare sector has posed new technological challenges to miniaturize and embed standard medical equipment in wearable devices [1], [2]. Those mainly aim to provide systems for self-care monitoring, remote diagnosis, sports medicine, rehabili-

tation, and prosthetics [3], [4], [5]. In this frame of e-health, temperature sensors acquired great relevance in order to control the course of infective disease, illnesses, and wound healing [6], [7], [8], [9] as well as improve the state-of-the-art accuracy of commercial devices [10]. Moreover, in prosthetics, the possibility to embed temperature sensors can address two different needs: 1) it improves the haptic information that can be collected from the environment providing accurate feedback to the user [11] and 2) it enhances the detection of environmental temperature as an influence factor on the performance of other sensors, which allows compensating for its effect [12], [13], [14], [15], [16], [17], [18].

Different kinds of temperature sensors can be found in the literature, each with their unique capabilities and limitations. A first class is based on semiconductors to form both pn junctions and/or transistor-like structures [19]. Those devices can also be based on organic semiconductors to achieve flexible and biocompatible devices [20]. Thermocouples, on the other hand, are based on the Seebeck effect and allow a precise detection of temperature gradients, but are not suitable for providing absolute temperatures. The use of positive/negative coefficient thermistors is also widespread. Those devices are

Manuscript received 8 March 2023; revised 22 May 2023; accepted 26 May 2023. Date of publication 12 June 2023; date of current version 1 August 2023. The associate editor coordinating the review of this article and approving it for publication was Prof. Gijs J. M. Krijnen. (Corresponding author: Tiziano Fapanni.)

Tiziano Fapanni, Dario Zappa, Emilio Sardini, and Mauro Serpelloni are with the Department of Information Engineering, University of Brescia, 25123 Brescia, Italy (e-mail: tiziano.fapanni@unibs.it).

Hatem ElBidweihy is with the Electrical and Computer Engineering Department, United States Naval Academy, Annapolis, MD 21402 USA.

Elisabetta Comini is with the Department of Information Engineering, University of Brescia, 25123 Brescia, Italy.

Digital Object Identifier 10.1109/JSEN.2023.3283797

nonlinear and are usually produced by rigid and non-easily printable materials [21]. On the other hand, resistive temperature detectors (RTDs) are based on the thermoresistive effect through which the resistance of a metal changes with temperature due to both a change in the resistivity of the bulk material and structural modifications. Such structural changes in metals are found to be negligible [22]. Among the possible different techniques that have been proposed in the literature for the fabrication of RTDs, printed and additive manufacturing techniques are reported. Those allow a quick prototyping process, can be adapted to work on nonplanar/3-D surfaces, and offer a wide range of compatible materials. All these capabilities are promising for the development of smart objects [23], [24]. Among the possible printed techniques, aerosol jet printing (AJP) is attractive because of its flexibility in terms of supported viscosity of the inks and its fully digital and maskless production process, which allows quick and economic prototyping that is ideal in the research frame. AJP basic principles have already been described in the literature [25]. In brief, the process is controlled by three gas flows. An atomizer flow is used to produce a mist from the liquid ink and to carry it toward the deposition nozzle, where the sheath flow focuses it on the substrate to avoid clogging events. The exhaust flow works to create a pressure difference in the impactor that allows selecting the dimensions of the particles suspended in the carrier flow and, thus, the characteristics of the printed line.

It is important to note that all the printed inks are usually composed of nanoparticles suspended in a set of solvents. In order to ensure proper electrical conductivity, it is, thus, important to propose a proper curing process that eliminates all the spurious matter and connects the nanoparticles in a homogeneous way. Ink producers usually provide recommended curing process parameters to achieve certain resistivity values. On the other hand, however, no data are usually provided with respect to the temperature coefficient of resistance (TCR) of the material. From these considerations, the aim of this work is to compare different curing temperatures within the curing range proposed by the producers, correlating the microscopic characteristics of the cured ink to the macroscopic ones (e.g., room temperature resistance and TCR) of the final device to improve the design process of fully printed RTDs.

II. MATERIALS AND METHODS

A. Sensor Design

The proposed study aims at evaluating the effect of curing or sintering temperatures on the conductive materials used in ink-based printed electronics. To avoid observing unwanted effects, such as resistance variation due to bending and stretching, a rigid material was selected as the substrate. The selected material is Al_2O_3 alumina because of its mechanical sturdiness and great ability to withstand high temperatures up to 1500 °C. For the functional materials, two well-known and widely used commercial nanoparticle-based inks were selected: silver (SmartAero, Genesink, Rousset, France) and gold (UTDAuTE, UTDOTS, Champaign, IL, USA). The sensors were then designed in order to maximize the length/area ratio, to provide easily accessible electrodes for wiring and to

TABLE I
PROCESS PARAMETERS SELECTED FOR THE
PRINTING OF THE TWO INKS

	Ag ink	Au ink
Sheath Flow (SCCM)	1240	90
Atomizer Flow (SCCM)	820	23
Exhaust Flow (SCCM)	800	--
UA current (mA)	--	635
Plate temperature (°C)	60	70
Printing speed (mm/s)	5	5
Deposition passes (#)	1	2
Nozzle Size (μm)	300	300

produce resistances of a few hundreds of ohms. In the design of the geometry of the sensors, no considerations were made in this study about the sensitivity to bending and the possible capacitive and inductive parasites, since the selected substrate is rigid and the temperature presents slow changing features that do not require high-frequency measurements.

This last specification was determined based on the inks' resistivity as well as the designed geometrical features. The initial design was used for preliminary printing tests in order to determine the optimal printing parameters, which were different due to the different composition and viscosity of the two inks. The main difference is the atomization process: the silver ink was atomized using the pneumatic atomizer, while the gold ink used the ultrasonic one. Thus, the former uses mainly the atomizer flow to atomize the ink, while the latter employs a piezoelectric device to perform this task. The ultrasonic atomizer is usually controlled by means of a current to determine the atomization power. The preliminary tests indicated that multiple ink deposition passes are required to achieve acceptable conductivity values for the gold ink. Thus, to achieve similar printing times and resistances in the same order of magnitude for the two inks, the gold sample design was scaled down. Images of the general dimensions of the silver and gold devices printed are shown in Fig. 1. For both inks, a six-sensor design on a single 2.5- × 2.5-in alumina substrate was printed using an aerosol jet printer (AJ300, Optomec, Albuquerque, USA) with the process parameters listed in Table I. Even though the two inks employ two different atomizers (ultrasonic for the Au ink and pneumatic for Ag ink) and, thus, required different process parameters, the production process is the same. First, the substrates were thoroughly cleaned with ethanol to remove dust particles, grease, and any kind of dirt. Then, all the samples were printed in series to reduce the printing variability. For each ink, five samples were produced (30 sensors for each ink in total). In order to evaluate the differences in the samples due to the curing temperature, each one was cured at a different temperature within the curing range proposed by the ink manufacturers. The selected curing temperatures are reported in Table II. After the sample fabrication, they were left on the deposition plate that was kept heated for 15 min in order to dry. After that, the samples were moved and left cooling down to environmental temperature before placing them in a ThermoScientific VACUTherm Oven (Thermo Electron LED GmbH, Langensfeld, Germany). Then, the selected curing

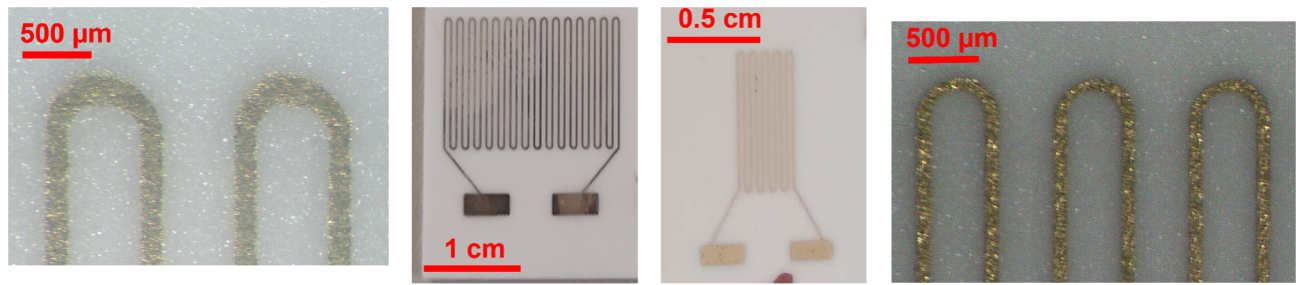


Fig. 1. Example of the produced silver (left) and gold (right) electrodes.

TABLE II
CURING TEMPERATURE FOR EACH OF THE PRODUCED
SAMPLES FOR BOTH SILVER AND GOLD

	S1	S2	S3	S4	S5
Silver	100°C	120°C	150°C	200°C	250°C
Gold	275°C	300°C	325°C	350°C	375°C

temperature was set and reached from room temperature following an 8 °C/min ramping profile. The target temperature was kept fixed for 60 min before switching off the oven and removing the samples when the temperature reached 100 °C. This curing process was conducted at environmental atmosphere for all the sensors. After the curing process, all the sensors on each sample were evaluated at room temperature to assess the quality of the printing and curing processes. A set of visual evaluations was carried on with an optical microscope (NB50T, Orma Scientific, Sesto San Giovanni, Milan, Italy) to measure the linewidth of the printed sensors. The room temperature resistance was measured using a Hewlett–Packard 34401a (HP, Palo Alto, CA, USA) digital multimeter in a four-wire configuration. After those preliminary tests, the sensors were connected in a four-wire configuration to a set of wires that were soldered using a two-part silver-based conductive epoxy (CW2400, Chemtronics, Kennesaw, USA). After its application, the epoxy was oven-cured at 80 °C for 60 min.

B. SEM Imaging

Morphological investigations were carried out using a field-emission scanning electron microscope (FE-SEM) MIRA-3 (TESCAN, Brno, Czech Republic) at an accelerating voltage of 5–7 kV to assess the differences produced by the different curing processes and selected ink. The samples were analyzed at different magnification values to evaluate the different features in the microscopic disposition of the nanoparticles as well as their agglomeration due to the curing process. Then, the images were elaborated using ImageJ software to evaluate the particle/pores size. After annotating the required scale to each image, the images were enhanced with the software to increase the visibility of the particles. Then, the area of the particles was extracted and statistically analyzed.

C. Temperature Sensitivity Evaluation

In order to evaluate the behavior of the sensors at different temperatures, the sensors were placed inside a climatic chamber UC 150/70 (Advanced Material Testing S.R.L., Limbiate, Italy) programed to change the temperature in steps in the

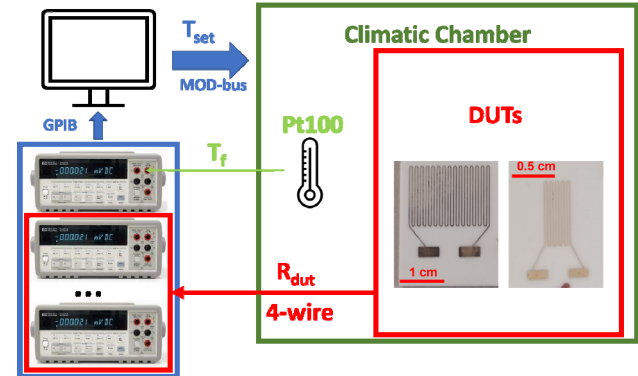


Fig. 2. Scheme of the experimental setup for the evaluation of the sensitivity to temperature. In brief, a computer mounting a dedicated LabVIEW VI was devoted to set the temperature set point (T_{set}) for the climatic chamber and to acquire the resistance of the device under test (DUT) from an array of HP34401a digital multimeters. A commercial temperature sensor was also measured to retrieve the actual temperature (T_f) in the proximity of the DUTs.

range between -10 °C and $+70$ °C. All the sensors were measured by a set of Hewlett–Packard 34401a (HP, Palo Alto, CA, USA) digital multimeters in a four-wire configuration controlled by a LabVIEW virtual instrument that sampled their readings at 1 Hz. Moreover, a Pt100 standard sample was also placed close to the samples to provide a known and fixed temperature reference for the measurements. The experimental setup is shown in Fig. 2.

The collected data were then processed using MATLAB. A simple code that identifies all the set-point temperatures was prepared and used to obtain statistical information on the resistance variation as well as to calculate the TCR in all the situations. The simplified characteristic equation (1) for RDT sensors defines R_0 as the resistance of the sensors at the temperature T_0 , R as the resistance of the sensors at temperature T , and α as the TCR of the sensors. Equation (1) is expanded to match the explicit equation of a line. Assuming $T_0 = 0$ and defining $T - T_0 = \Delta T$ as the independent variable, the collected data points were fit to a line, and the two obtained parameters (m as slope and q as intercept) were matched to the ones obtained in (1) obtaining the system in (2)

$$R = R_0 \cdot [1 + \alpha (T - T_0)] = R_0 \cdot [1 + \alpha \Delta T] = \alpha \Delta T R_0 + R_0 \quad (1)$$

$$\begin{cases} m &= \alpha R_0 \\ q &= R_0. \end{cases} \quad (2)$$

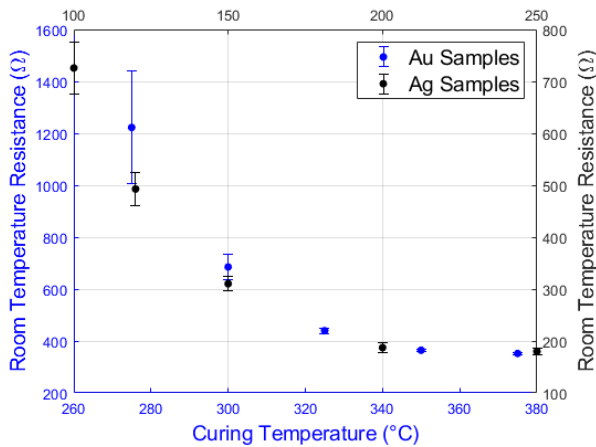


Fig. 3. Room temperature resistance variation on the samples produced both by silver and gold ink.

The obtained TCRs were then compared and evaluated to determine differences in behavior due to the curing process and selected material.

III. RESULTS AND DISCUSSION

A. Printing Process Evaluation

After the printing process, all the samples underwent an accurate microscopical analysis that allowed the evaluation of the printed linewidth. A few examples of the printed sensors with details captured by the microscope are reported in Fig. 1. The silver ink produced on average a linewidth of $(116 \pm 9) \mu\text{m}$, while the gold ink produced a thinner line on average of $(77 \pm 7) \mu\text{m}$. Those differences are related to the different processes employed in the production step and the different properties of the inks. Even though there were differences in the production parameters, the obtained lines were uniform in width without sensible difference between the samples and between the two selected inks. Then, the room temperature resistance was evaluated on all the samples for both functional inks. The measured resistance values of the five samples cured at different temperatures are shown in Fig. 3. In general, the overall resistance decreases when the curing temperature increases, indicating an improved conductivity. Moreover, the overall variability within the samples (evaluated by calculating the coefficient of variation) tends to decrease. According to the collected data, the overall variability was halved in the silver ink samples (from 6.83% down to 3.09%), while it was reduced from 17.76% down to 0.89% in the gold ink ones. However, in the latter situation, a slight increase in the coefficient of variation was observed at the last curing temperature. This effect may be due to excessive thermal stress induced on the printed tracks that leads to random cracking and, thus, to higher variability [26].

B. SEM Imaging

The SEM images showed microscopic features that allowed better understanding of the different degrees of sinterization of the inks related to the applied curing temperatures. The silver ink shows clear differences in the nanoparticle agglomeration

pattern (Fig. 4). Below 120 °C, the nanoparticles do not present great differences and appear to be almost unchanged. Raising the curing temperature up to 150 °C, the nanoparticles start to agglomerate and fuse with one another creating bigger clusters. At 200 °C, the particles start to appear increasingly more uniform and agglomerated, presenting, however, a set of holes. For the gold ink (Fig. 5), the behavior seems similar to the one already described for the silver ink. In particular, at the first tested curing temperature (275 °C), the nanoparticles are clearly visible, while they cluster in bigger groups as the curing temperature increases. The cluster size seems to reach a plateau after 325 °C. Those visual evaluations were confirmed and quantified through ImageJ software that allowed the estimation of the particle sizes. The achieved results for silver and gold samples are shown in Figs. 4(f) and 5(f), respectively.

C. Temperature Sensitivity Evaluation

The temperature sensitivity was evaluated on five sensors for each sample in the climatic chamber described in Section II-C. The results of those experiments are shown in Fig. 6. The silver ink samples [Fig. 6(c)] show a linear correlation ($R^2 = 0.991$) between TCR and the curing temperature. On the other hand, the gold ink samples [Fig. 6(d)] show a TCR that initially rises with the curing temperature but then reaches a plateau when cured at 325 °C or above. The cured silver ink shows TCR values that are comparable to that of bulk silver reported in the literature [27] ($\approx 3.8 \times 10^{-3} \text{ }^\circ\text{C}^{-1}$), while the cured gold ink reaches a maximum TCR value of around $2.5 \times 10^{-3} \text{ }^\circ\text{C}^{-1}$, lower than that of bulk gold ($\approx 3.7 \times 10^{-3} \text{ }^\circ\text{C}^{-1}$). The TCR results in this section can be correlated with SEM images in Section III-B to reveal the relationship between the microscopic agglomeration of the nanoparticles and the macroscopic characteristics of the printed devices.

IV. DISCUSSION

In this work, the microscopic and macroscopic properties of two commercial nanoparticle-based inks have been evaluated at different curing temperatures. SEM images as well as room temperature resistance and TCR have been collected and analyzed for various samples. The sensors were designed as simple serpentes and then preliminary evaluated to assess the achieved linewidth and the room temperature resistance. The overall linewidth presented small variations both using the silver ($\text{CV}_{\text{Ag}} = 7.7\%$) and the gold ($\text{CV}_{\text{Au}} = 9.1\%$) inks considering all the produced sensors. The room temperature resistance, on the other hand, presents a reduction of 71.2% for the gold samples and 75.2% for the silver ones with increasing curing temperatures. A considerable decrease in the coefficient of variation of the room temperature resistance at rising curing temperatures up to 95% is observed, which indicates how curing the inks at higher temperatures tends to uniform the variability of the produced sensors. Moreover, on the macroscopic scale, the behavior in temperature of the sensors was evaluated by means of a climatic chamber in the $[-10 \text{ }^\circ\text{C}; 70 \text{ }^\circ\text{C}]$ temperature range. This evaluation produced

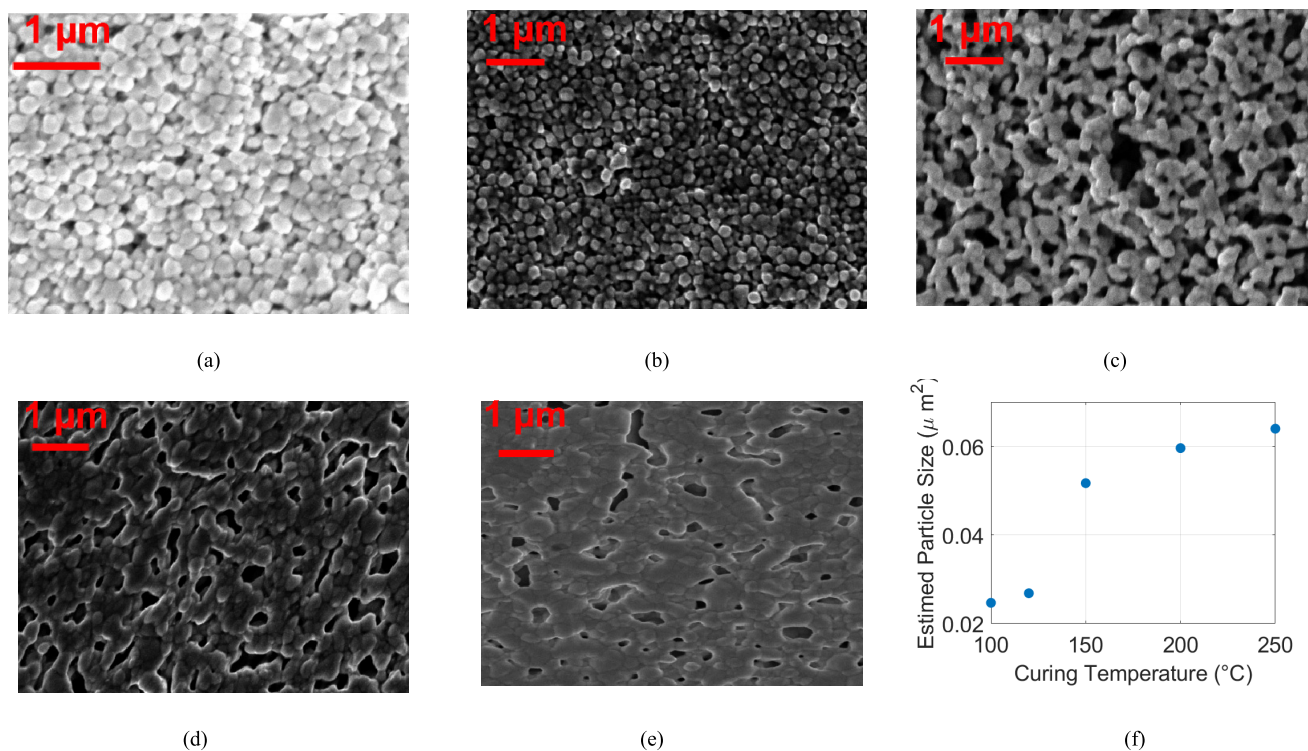


Fig. 4. Results of the SEM evaluation performed on the silver samples cured at (a) 100 $^{\circ}\text{C}$, (b) 120 $^{\circ}\text{C}$, (c) 150 $^{\circ}\text{C}$, (d) 200 $^{\circ}\text{C}$, and (e) 250 $^{\circ}\text{C}$. In (f), the estimated cluster size is plotted with respect to the curing temperature.

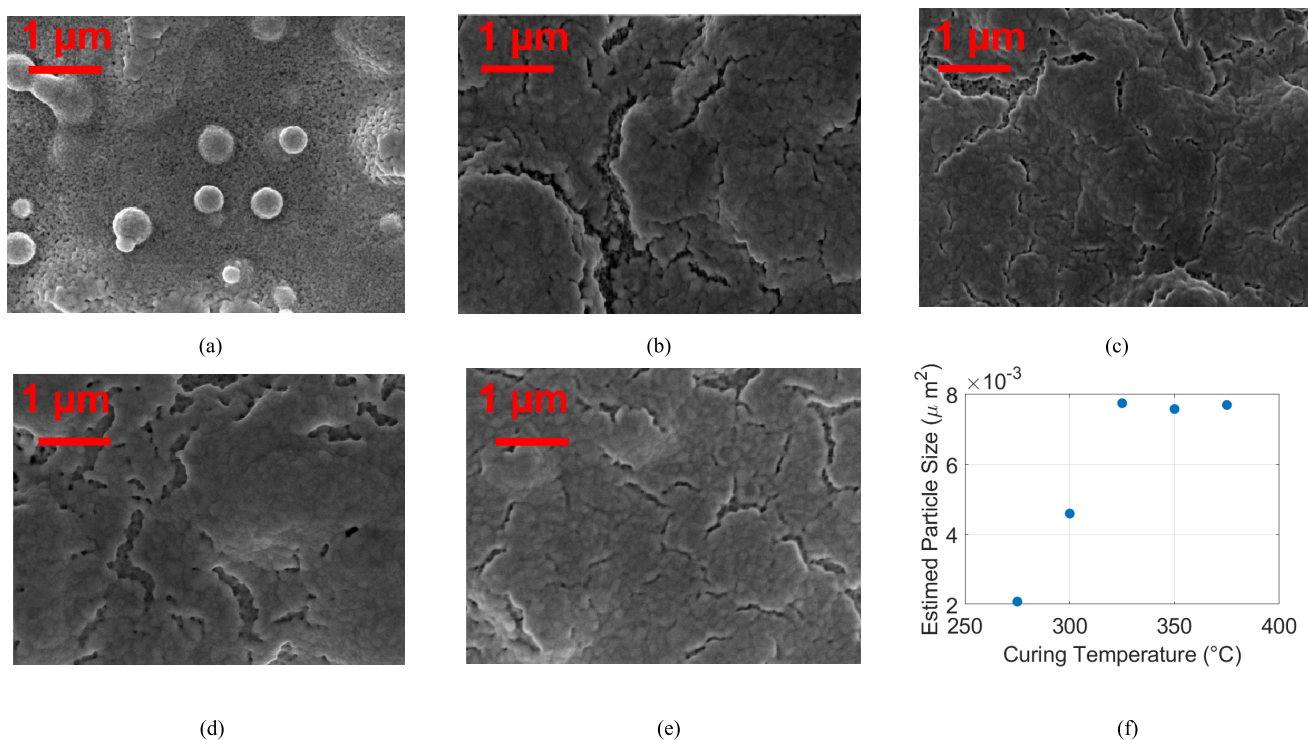


Fig. 5. Results of the SEM evaluation performed on the gold samples cured at (a) 275 $^{\circ}\text{C}$, (b) 300 $^{\circ}\text{C}$, (c) 325 $^{\circ}\text{C}$, (d) 350 $^{\circ}\text{C}$, and (e) 375 $^{\circ}\text{C}$. In (f), the estimated cluster size is plotted with respect to the curing temperature.

for the silver sample an increasing sensitivity with increasing curing temperatures, with TCRs that reached values up to $3.4 \times 10^{-3} \text{ }^{\circ}\text{C}^{-1}$. On the other hand, the TCR of the gold

samples reached a plateau at around $2.5 \times 10^{-3} \text{ }^{\circ}\text{C}^{-1}$ for all the samples cured at temperatures above 325 $^{\circ}\text{C}$. The SEM images allowed the understanding of the different nanoparticle

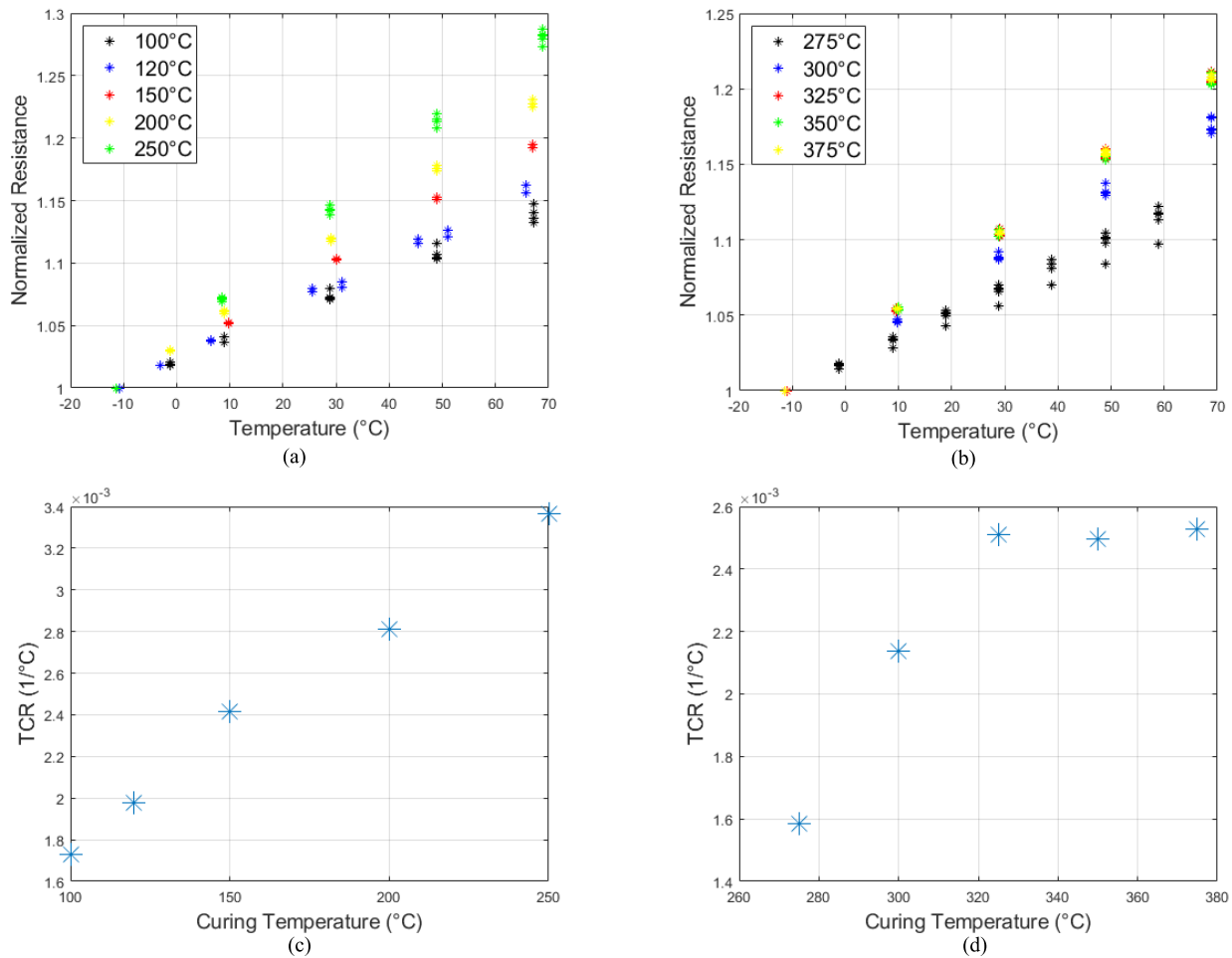


Fig. 6. Calibration relationship achieved with (a) silver and (b) gold ink at different curing temperatures. The different TCRs obtained after the different curing temperatures were reported in (c) for silver and (d) for gold ink.

clustering achieved with the proposed curing temperatures. The silver ink tends to increase almost linearly the particle size up to 61.5% until it reaches a bulk-like configuration, which, however, presents a set of cavities. Gold nanoparticles, on the other hand, present a plateau in the cluster size after an increase of 71.0% the size. Those microscopic characteristics seem to reflect the macroscopic behavior of the sensitivity of the overall sensors in temperature. As suggested in [28] for the overall resistivity, this result is related to the different cluster sizes and to the number of boundaries between the different grains.

The differences between the two inks are, thus, mostly related to the different curing parameters that allow different aggregation of the particles. In fact, as reported in the literature [29], the melting temperature of a material is dependent both to the particle size and to the material itself with silver having lower melting temperature than gold [30], [31].

V. CONCLUSION

In conclusion, in this work, the behavior of two materials was analyzed both from the microscopic and macroscopic points of view. The achieved results underline the need to study the effects of the curing process for any material used in

additive manufacturing as a powerful process parameter to be considered when designing sensors or systems. In particular, it was observed how the microscopic structure of the materials, that is, directly related to the curing temperature, impact on the macroscopic characteristics of the sensor, such as its TCR and its room temperature resistance. In general, the former tends to increase at rising curing temperature, while the latter decreases. This information implies an increase in the sensitivity of the material, but at the same time a possible decrease in the absolute sensitivity of the sensor. It must be noted, however, that increasing the curing temperature also highly reduces the process variability and, thus, increases its repeatability. On the other hand, increasing the curing temperature over the maximum suggested by the materials manufacturers can lead to the material degradation due to the formation of mechanical stresses in the structure and the evaporation of the functional material. Another constraint that has to be considered when selecting the curing temperature is related to the selected substrate that must be able to withstand the curing process. Future work will take into account the hereby presented results in order to improve the design of fully printed temperature sensors and their interconnections to enhance their metrological characteristics

and better meet custom and application-specific requirements as well as furtherly reducing the costs, as well as to try to better investigate other characteristics, such as the stability over time of the sensitivity and the performance consistency with quick temperature changes.

REFERENCES

- [1] S. Zhang, S. Li, Z. Xia, and K. Cai, "A review of electronic skin: Soft electronics and sensors for human health," *J. Mater. Chem. B*, vol. 8, no. 5, pp. 852–862, 2020, doi: [10.1039/c9tb02531f](https://doi.org/10.1039/c9tb02531f).
- [2] K. K. Yeung, T. Huang, Y. Hua, K. Zhang, M. M. F. Yuen, and Z. Gao, "Recent advances in electrochemical sensors for wearable sweat monitoring: A review," *IEEE Sensors J.*, vol. 21, no. 13, pp. 14522–14539, Jul. 2021, doi: [10.1109/JSEN.2021.3074311](https://doi.org/10.1109/JSEN.2021.3074311).
- [3] A.-C. Bunea et al., "E-skin: The dawn of a new era of on-body monitoring systems," *Micromachines*, vol. 12, no. 9, p. 1091, Sep. 2021, doi: [10.3390/mi12091091](https://doi.org/10.3390/mi12091091).
- [4] E. Cantu et al., "Printed multi-EMG electrodes on the 3D surface of an orthosis for rehabilitation: A feasibility study," *IEEE Sensors J.*, vol. 21, no. 13, pp. 14407–14417, Jul. 2021, doi: [10.1109/JSEN.2021.3059308](https://doi.org/10.1109/JSEN.2021.3059308).
- [5] S. Tonello et al., "Preliminary study of a flexible printed multi-sensing platform for electromyography and lactate measuring during rehabilitation," in *Proc. IEEE Int. Symp. Med. Meas. Appl. (MeMeA)*, Jun. 2021, pp. 1–6, doi: [10.1109/MeMeA52024.2021.9478729](https://doi.org/10.1109/MeMeA52024.2021.9478729).
- [6] H. S. Jeon, J. H. Kim, M. B. G. Jun, and Y. H. Jeong, "Fabrication of thermochromic membrane and its characteristics for fever detection," *Materials*, vol. 14, no. 13, p. 3460, Jun. 2021, doi: [10.3390/ma14133460](https://doi.org/10.3390/ma14133460).
- [7] Y. Zhang et al., "Flexible integrated sensing platform for monitoring wound temperature and predicting infection," *Microbial Biotechnol.*, vol. 14, no. 4, pp. 1566–1579, Jul. 2021, doi: [10.1111/1751-7915.13821](https://doi.org/10.1111/1751-7915.13821).
- [8] A. Al-Halhouli, A. Albagdady, J. Alawadi, and M. A. Abeeleh, "Monitoring symptoms of infectious diseases: Perspectives for printed wearable sensors," *Micromachines*, vol. 12, no. 6, p. 620, 2021, doi: [10.3390/mi12060620](https://doi.org/10.3390/mi12060620).
- [9] M. Jose, G. Oudebrouckx, S. Bormans, P. Veske, R. Thoelen, and W. Deferme, "Monitoring body fluids in textiles: Combining impedance and thermal principles in a printed, wearable, and washable sensor," *ACS Sensors*, vol. 6, no. 3, pp. 896–907, Mar. 2021, doi: [10.1021/acssens.0c02037](https://doi.org/10.1021/acssens.0c02037).
- [10] G. I. Gasim, I. R. Musa, M. T. Abdien, and I. Adam, "Accuracy of tympanic temperature measurement using an infrared tympanic membrane thermometer," *BMC Res. Notes*, vol. 6, no. 1, pp. 2–6, Dec. 2013, doi: [10.1186/1756-0500-6-194](https://doi.org/10.1186/1756-0500-6-194).
- [11] J. Neto, R. Chirila, A. S. Dahiya, A. Christou, D. Shakthivel, and R. Dahiya, "Skin-inspired thermoreceptors-based electronic skin for biomimicking thermal pain reflexes," *Adv. Sci.*, vol. 9, no. 27, 2022, Art. no. 2201525, doi: [10.1002/advs.202201525](https://doi.org/10.1002/advs.202201525).
- [12] J. Huang et al., "Editors' choice—Review—Impedance response of porous electrodes: Theoretical framework, physical models and applications," *J. Electrochem. Soc.*, vol. 167, no. 16, Dec. 2020, Art. no. 166503, doi: [10.1149/1945-7111/abc655](https://doi.org/10.1149/1945-7111/abc655).
- [13] G. Wolterink, R. Sanders, F. Muijzer, B. J. Van Beijnum, and G. Krijnen, "3D-printing soft sEMG sensing structures," in *Proc. IEEE Sensors*, Oct. 2017, pp. 1–3, doi: [10.1109/ICSENS.2017.8233935](https://doi.org/10.1109/ICSENS.2017.8233935).
- [14] K. Kim et al., "Low-voltage, high-sensitivity and high-reliability bimodal sensor array with fully inkjet-printed flexible conducting electrode for low power consumption electronic skin," *Nano Energy*, vol. 41, pp. 301–307, Nov. 2017, doi: [10.1016/j.nanoen.2017.09.024](https://doi.org/10.1016/j.nanoen.2017.09.024).
- [15] P. S. Das and J.-Y. Park, "A flexible touch sensor based on conductive elastomer for biopotential monitoring applications," *Biomed. Signal Process. Control*, vol. 33, pp. 72–82, Mar. 2017, doi: [10.1016/j.bspc.2016.11.008](https://doi.org/10.1016/j.bspc.2016.11.008).
- [16] M. Chung, G. Fortunato, and N. Radacs, "Wearable flexible sweat sensors for healthcare monitoring: A review," *J. Roy. Soc. Interface*, vol. 16, no. 159, Oct. 2019, Art. no. 20190217, doi: [10.1098/rsif.2019.0217](https://doi.org/10.1098/rsif.2019.0217).
- [17] G. Li, S. Liu, Q. Mao, and R. Zhu, "Multifunctional electronic skins enable robots to safely and dexterously interact with human," *Adv. Sci.*, vol. 9, Apr. 2022, Art. no. 2104969, doi: [10.1002/advs.202104969](https://doi.org/10.1002/advs.202104969).
- [18] T. Fapanni, M. Serpelloni, and E. Sardini, "Uncertainty sources in aerosol jet printed and flexible electrochemical sensors," in *Proc. IEEE Int. Workshop Metrology Ind. 4.0 IoT*, Jun. 2022, pp. 245–249, doi: [10.1109/MetroInd4.0IoT54413.2022.9831522](https://doi.org/10.1109/MetroInd4.0IoT54413.2022.9831522).
- [19] M. Kimura and K. Toshima, "Thermistor-like pn junction temperature-sensor with variable sensitivity and its combination with a micro-air-bridge heater," *Sens. Actuators, A, Phys.*, vol. 108, nos. 1–3, pp. 239–243, 2003, doi: [10.1016/S0924-4247\(03\)00290-5](https://doi.org/10.1016/S0924-4247(03)00290-5).
- [20] J. Polena, D. Afzal, J. H. L. Ngai, and Y. Li, "Temperature sensors based on organic field-effect transistors," *Chemosensors*, vol. 10, no. 1, p. 12, Dec. 2021, doi: [10.3390/chemosensors10010012](https://doi.org/10.3390/chemosensors10010012).
- [21] J. Chen, Y. Zhu, Z. Guo, and A. G. Nasibulin, "Recent progress on thermo-electrical properties of conductive polymer composites and their application in temperature sensors," *Engineered Sci.*, vol. 12, pp. 13–22, Aug. 2020, doi: [10.30919/es8d1129](https://doi.org/10.30919/es8d1129).
- [22] T. Dinh, H. Phan, A. Qamar, P. Woodfield, N. Nguyen, and D. V. Dao, "Thermoresistive effect for advanced thermal sensors: Fundamentals, design considerations, and applications," *J. Microelectromech. Syst.*, vol. 26, no. 5, pp. 966–986, Oct. 2017, doi: [10.1109/JMEMS.2017.2710354](https://doi.org/10.1109/JMEMS.2017.2710354).
- [23] P. Bellitti, M. Borghetti, E. Cantu, E. Sardini, and M. Serpelloni, "Resistive sensors for smart objects: Analysis on printing techniques," *IEEE Trans. Instrum. Meas.*, vol. 71, pp. 1–15, 2022, doi: [10.1109/TIM.2022.3181941](https://doi.org/10.1109/TIM.2022.3181941).
- [24] M. Borghetti, E. Cantu, E. Sardini, and M. Serpelloni, "Printed sensors for smart objects in Industry 4.0," in *Proc. IEEE 6th Int. Forum Res. Technol. Soc. Ind. (RTSI)*, Sep. 2021, pp. 57–62, doi: [10.1109/RTSI50628.2021.9597209](https://doi.org/10.1109/RTSI50628.2021.9597209).
- [25] M. Borghetti, E. Cantu, E. Sardini, and M. Serpelloni, "Future sensors for smart objects by printing technologies in Industry 4.0 scenario," *Energies*, vol. 13, no. 22, p. 5916, Nov. 2020, doi: [10.3390/en13225916](https://doi.org/10.3390/en13225916).
- [26] M. Serpelloni, E. Cantu, M. Borghetti, and E. Sardini, "Printed smart devices on cellulose-based materials by means of aerosol-jet printing and photonic curing," *Sensors*, vol. 20, no. 3, p. 841, Feb. 2020, doi: [10.3390/s20030841](https://doi.org/10.3390/s20030841).
- [27] R. Serway, *Principles of Physics*. Fort Worth, TX, USA: Saunders College, 1998.
- [28] M. T. Rahman, J. McCloy, C. V. Ramana, and R. Panat, "Structure, electrical characteristics, and high-temperature stability of aerosol jet printed silver nanoparticle films," *J. Appl. Phys.*, vol. 120, no. 7, Aug. 2016, Art. no. 075305, doi: [10.1063/1.4960779](https://doi.org/10.1063/1.4960779).
- [29] F. Font and T. G. Myers, "Spherically symmetric nanoparticle melting with a variable phase change temperature," *J. Nanoparticle Res.*, vol. 15, no. 12, pp. 1–13, Dec. 2013, doi: [10.1007/s11051-013-2086-3](https://doi.org/10.1007/s11051-013-2086-3).
- [30] M. Asoro, J. Damiano, and P. Ferreira, "Size effects on the melting temperature of silver nanoparticles: In-situ TEM observations," *Microsc. Microanal.*, vol. 15, pp. 706–707, Jul. 2009, doi: [10.1017/S1431927609097013](https://doi.org/10.1017/S1431927609097013).
- [31] Z. Qiao, H. Feng, and J. Zhou, "Molecular dynamics simulations on the melting of gold nanoparticles," *Phase Transitions*, vol. 87, no. 1, pp. 59–70, Jan. 2014, doi: [10.1080/01411594.2013.798410](https://doi.org/10.1080/01411594.2013.798410).

Tiziano Fapanni received the M.Sc. (cum laude) degree in electronic engineering from the University of Brescia, Brescia, Italy, in 2019, and the Ph.D. degree from the Department of Information Engineering, University of Brescia, in 2023.

His research interests include the development of sensors and conditioning circuit for e-skin application to monitor physiological and biochemical signals.

Hatem ElBidweihy received the B.S. and M.S. degrees in electrical power systems from Cairo University, Cairo, Egypt, in 2009 and 2011, respectively.

He is an Associate Professor of Electrical and Computer Engineering at the United States Naval Academy, Annapolis, MD, USA. He is the Director of the Microfabrication and Rapid Prototyping Laboratory at United States Naval Academy. His current research interests include additive manufacturing of flexible and stretchable electronics.

Dario Zappa received the B.Sc. and M.Sc. degrees in electronic engineering and the Ph.D. degree in material science from the University of Brescia, Brescia, Italy, in 2006, 2009, and 2013, respectively.

In 2014, he worked as a Researcher at Consiglio Nazionale delle Ricerche - Istituto Nazionale di Ottica (CNR-INO), University of Brescia, and in 2017, he was appointed as an Assistant Professor at the University of Brescia. In 2022, he became an Associate Professor at the Department of Information Engineering, University of Brescia. At the SENSOR Lab, Brescia, his research activities focused on the synthesis and characterization (morphological, structural, and functional) of nanostructured materials, including metal oxides and dichalcogenides, for different applications, ranging from chemical sensors, e-noses, solid oxide fuel cells (SOFC), and thermoelectric devices. In the last few years, he was involved in many international projects (European Union (EU): "Oxide Materials Towards a Matured Post-silicon Electronics Era (ORAMA)," "surface ionization and novel concepts in nano-MOX gas sensors with increased selectivity, sensitivity and stability for detection of low concentrations of toxic and explosive agents (S3)," and "sniffer for concealed people discovery (SNOOPY)"; North Atlantic Treaty Organization (NATO): "advanced metal Oxides and heterostructures for electro-optical chemical sensors (AMOXES)," Italy-Korea and Italy-Singapore Bilateral projects) and in some national projects (Piano Nazionale di Ripresa e Resilienza (PNRR), Ministero dell'Istruzione, dell'Università e della Ricerca - Fondo per gli Investimenti della Ricerca di Base (MIUR-FIRB), and Regione Lombardia). Since 2012, he has been a Lecturer in physics at the University of Brescia. His Hirsch index (H-index) is 23 and has over 1900 citations on Scopus.

Elisabetta Comini received the degree in physics from the University of Pisa, Pisa, Italy, in 1996, and the Ph.D. degree in material science from the University of Brescia, Brescia, Italy, in 2000.

In 2001, she was appointed as an Assistant Professor of Physics of Matter at the University of Brescia, where she became a Full Professor in 2016. She has been an organizer of several symposia in the sensing field for MRS and European Materials Research Society (E-MRS). She is currently a Full Professor. She is a researcher specialist in the growth of metal oxides, particularly nanowires, thin films, and the measurement of their electronic, functional, and structural properties. She is the Director of the SENSOR Laboratory, University of Brescia (<http://sensor.unibs.it>), and the Co-Founder of Nano sensor systems (NASYS), Via Alfredo Catalani, Reggio Emilia, Italy. She has more than 430 peer-reviewed papers and an H-index of 61 [Web of Science (WoS)], 63 (Scopus), and 71 (Google Scholar). Her papers are cited widely around the world; citations are 14 926 (WoS), 16 287 (Scopus), and 21 061 (Google Scholar). Moreover, she has filed five patents.

Dr. Comini has been nominated as a EUROSENSORS 2012 Fellow. She was selected as a Vebleo Fellow in 2020. She has received several awards at the Eurosensors Conference and MRS. She has been selected among the top-100 Italian women scientists. She is ranked first in the Top Italian Women Scientists Material and Nano Sciences list and among the top 20 in the Top Italian Scientists Material and Nano Sciences list. She was the Chair of the MRS Fall Meeting 2013.

Emilio Sardini (Member, IEEE) received the M.Sc. degree in electronics engineering from the Politecnico di Milano, Milan, Italy, in 1983.

He is currently a Full Professor with the Department of Information Engineering, University of Brescia, Brescia, Italy. He has been a member of the Academic Senate, the Board of Directors of the University of Brescia, the Deputy Dean of the Engineering Faculty, the Director of the Department of Information Engineering, University of Brescia, and the Coordinator of the "Technology for Health" Ph.D. Program. His research interests include electronic instrumentation, sensors and signal conditioning electronics, and development of autonomous sensors for biomedical applications.

Mauro Serpelloni (Senior Member, IEEE) received the M.S. (cum laude) degree in industrial management engineering and the Ph.D. degree in electronic instrumentation from the University of Brescia, Brescia, Italy, in 2003 and 2007, respectively.

He is currently a Full Professor of Measurements with the Department of Information Engineering, University of Brescia. His current research interests include printed sensors, contactless transmission and signal processing for measurement systems, sensors for biosignals, and wearable devices.